HAL
open science

Detecting nanoparticles at radio frequencies: Jovian dust stream impacts on Cassini/RPWS

Nicole Meyer, Alain Lecacheux, Michael L. Kaiser, Donald A. Gurnett

To cite this version:

Nicole Meyer, Alain Lecacheux, Michael L. Kaiser, Donald A. Gurnett. Detecting nanoparticles at radio frequencies: Jovian dust stream impacts on Cassini/RPWS. Geophysical Research Letters, 2009, 36, pp.03103. 10.1029/2008GL036752 . hal-03785259

HAL Id: hal-03785259

https://hal.science/hal-03785259v1

Submitted on 21 Oct 2022

HAL is a multi-disciplinary open access archive for the deposit and dissemination of scientific research documents, whether they are published or not. The documents may come from teaching and research institutions in France or abroad, or from public or private research centers.

L'archive ouverte pluridisciplinaire **HAL**, est destinée au dépôt et à la diffusion de documents scientifiques de niveau recherche, publiés ou non, émanant des établissements d'enseignement et de recherche français ou étrangers, des laboratoires publics ou privés.

Copyright

19448007, 2009, 3, Downloaded from https://agupubs.onlinelibrary.wiley.com/doi/10.1029/2008GL036752 by Cochrane France, Wiley Online Library on [21/10/2022]. See the Terms and Conditions (https://onlinelibrary.wiley.com/terms-and-conditions) on Wiley Online Library for rules of use; OA articles are governed by the applicable Creative Commons License

Detecting nanoparticles at radio frequencies: Jovian dust stream impacts on Cassini/RPWS

N. Meyer-Vernet,[1] A. Lecacheux,[1] M. L. Kaiser,[2] and D. A. Gurnett[3]

Received 21 November 2008; accepted 31 December 2008; published 7 February 2009.

[1] We analyse wave observations by the Cassini/RPWS instrument performed during the Jovian fly-by, when the on-board dust analyser recorded dust streams which were interpreted as nanoparticles moving at about the solar wind speed. The observed wave pulses are produced by ionisation of dust grains impacting the spacecraft. Nanoparticles are detected because they move fast and the voltage produced by impact ionisation increases very fast with speed, so that they produce wave pulses as high as do much larger grains of smaller speeds. The observed wave level and spectral shape are compatible with those expected for the streams deduced from the dust analyser observations, and the impact rates observed on both instruments appear to vary similarly. The present result is the first wave detection simultaneous with a conventional detection by a dust analyser attributed to nanoparticles. **Citation:** Meyer-Vernet, N., A. Lecacheux, M. L. Kaiser, and D. A. Gurnett (2009), Detecting nanoparticles at radio frequencies: Jovian dust stream impacts on Cassini/RPWS, *Geophys. Res. Lett.*, *36*, L03103, doi:10.1029/2008GL036752.

1. Introduction

[2] Wave instruments are used routinely on space missions to measure in situ the electron density and temperature in various environments, using quasi-thermal noise spectroscopy [*Meyer-Vernet et al.*, 1998]. That wave instruments can also be used for measuring dust was realized when both the radio [*Warwick et al.*, 1982] and plasma wave [*Scarf et al.*, 1982] instruments on the Voyager 2 spacecraft, which did not carry conventional dust analysers, detected dust grains in Saturn's G ring. This serendipitous observation opened the way to a novel technique for measuring dust with wave instruments, which has been subsequently applied in various environments [see *Meyer-Vernet*, 2001], including recent observations of large grains near Saturn with the radio and plasma wave science (RPWS) instrument on Cassini [*Kurth et al.*, 2006], and the recent discovery of nanoparticles accelerated by the solar wind motional electric field at 1 AU, with the STEREO/WAVES instrument [*Meyer-Vernet et al.*, 2008].

[3] When a dust particle impacts a solid target at a velocity greater than the sound speed in the materials - typically a few km/s - it undergoes a strong shock compression which vaporises and ionises it as well as a part of the target. This material expands and the residual charge [*Drapatz and Michel*, 1974] produces an electric pulse which is detected by the antennas - a process akin to that used by grain mass spectrometers in space [*Göller and Grün*, 1989].

[4] Even though wave detection of dust is affected by a large uncertainty due to the badly known relation between the released charge and the grain properties, it has two major advantages which make it complementary to conventional dust detectors: first it has a much larger collecting area, which can be the whole spacecraft, and second, it is much less reliant on a specific spacecraft attitude for dust detection.

[5] In the present paper, we analyse the wave power spectral density measured with Cassini/RPWS when the on-board dust analyser detected dust streams made of nanoparticles, during the distant Jupiter fly-by of closest approach 138 R_J. Dust streams coming from Jupiter were discovered by the Ulysses dust analyser [*Grün et al.*, 1992], and later recognised from theoretical arguments as made of nanoparticles moving at several hundred km/s [*Zook et al.*, 1996], i.e., about 10^3 less massive and 5–10 times faster than originally reported; further analysis and detections by the Galileo and Cassini dust instruments suggested that these particles move still faster.

[6] These streams are attributed to ejection by Io of nanoparticles [*Graps et al.*, 2000], which are charged positively in Jupiter's magnetosphere because of secondary electron emission, accelerated outwards by the corotational electric field [*Johnson et al.*, 1980; *Horányi et al.*, 1997], and further accelerated by the solar wind motional electric field. Joint measurements by the dust detectors of Cassini and Galileo have revealed the properties of the dust impacting Cassini on December 29, 2000 [*Graps et al.*, 2001], enabling us to compare with wave observations.

2. Wave Observations

[7] The observations were carried out by the RPWS radio receivers [*Gurnett et al.*, 2004] connected to the electric antennas made of three 10-m booms mounted on the side of the spacecraft. We use the lowest filter of the high-frequency receiver, which covers the frequency range 3.5–15 kHz and can be connected in monopole (U, V, W) or dipole (U-V) mode, with the combinations [(U or V) and W] or [U-V and W] used sequentially.

[8] Figure 1 shows a radio spectrogram acquired during the Jovian flyby, displayed as frequency versus time, with relative intensity scaled in color as indicated. Impulsive wide-band signals of large-amplitude are clearly seen on 28–29 December 2000 and 4–5 January 2001, during periods marked in red on the spacecraft trajectory (Figure 1 (right)).

[1]LESIA, Observatoire de Paris, CNRS, Université Paris Diderot, Meudon, France.
[2]NASA Goddard Space Flight Center, Greenbelt, Maryland, USA.
[3]Department of Physics and Astronomy, University of Iowa, Iowa City, Iowa, USA.

Copyright 2009 by the American Geophysical Union.
0094-8276/09/2008GL036752

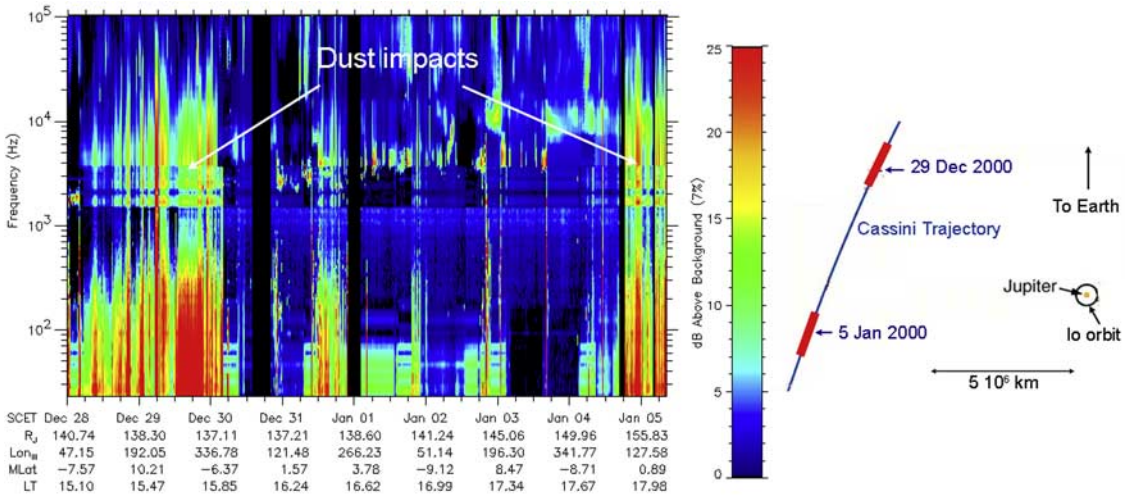

Figure 1. Radio spectrogram measured by Cassini/RPWS during the Jovian fly-by. The intervals of large impulse rates are marked in red on the spacecraft trajectory.

[9] Figure 2d shows the voltage power spectral density recorded at 4 kHz on the W antenna (43,000 spectra); we shall show below that the signal is similar on the other booms. Figures 2a–2c show the corresponding spectral shape at the times indicated, with each spectrum computed from waveform snapshots recorded during $\Delta t \sim 0.15$ s. The intense impulsive noise on Dec.29 (Figure 2a) and Jan.4 (Figure 2c) has a roughly f^{-4} spectrum above a few kHz, as

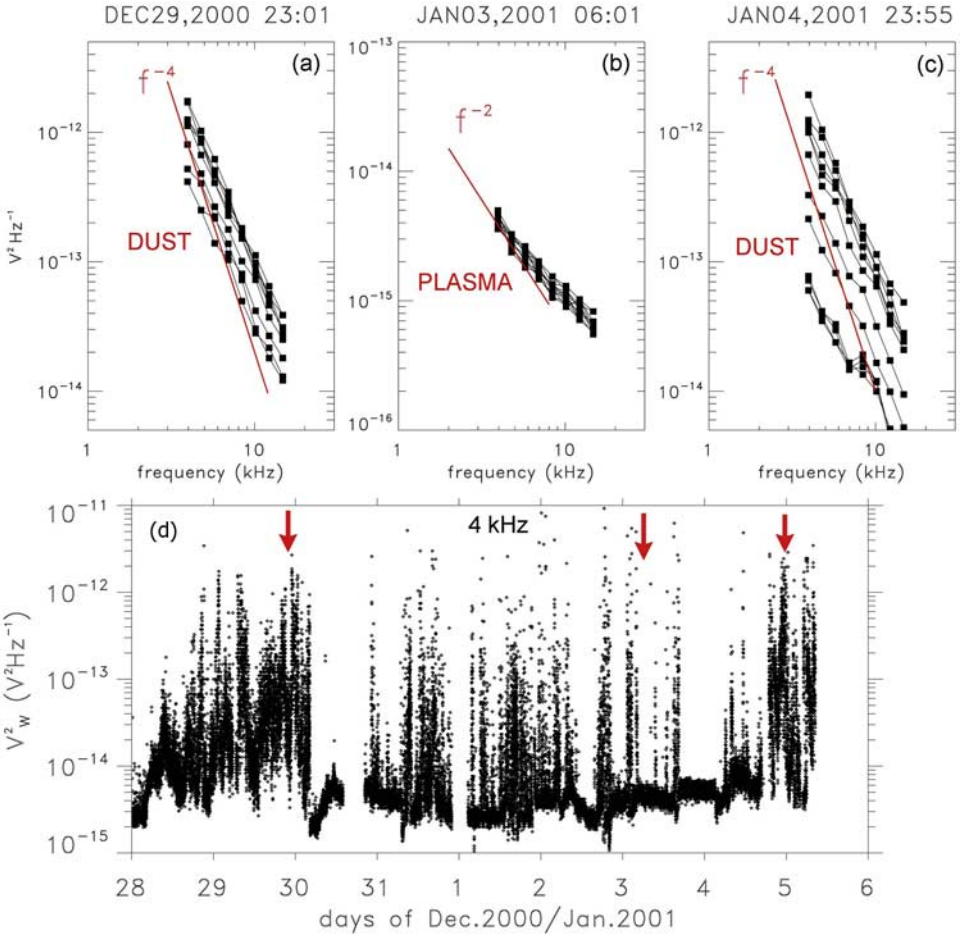

Figure 2. Bottom: power spectral density as a function of time recorded on the W antenna at 4 kHz. Top: with corresponding power spectra (computed from ~0.15 s snapshots) acquired during three 3 min. intervals centered at the times indicated.

19448007, 2009, 3, Downloaded from https://agupubs.onlinelibrary.wiley.com/doi/10.1029/2008GL036752 by Cochrane France, Wiley Online Library on [21/10/2022]. See the Terms and Conditions (https://onlinelibrary.wiley.com/terms-and-conditions) on Wiley Online Library for rules of use; OA articles are governed by the applicable Creative Commons License

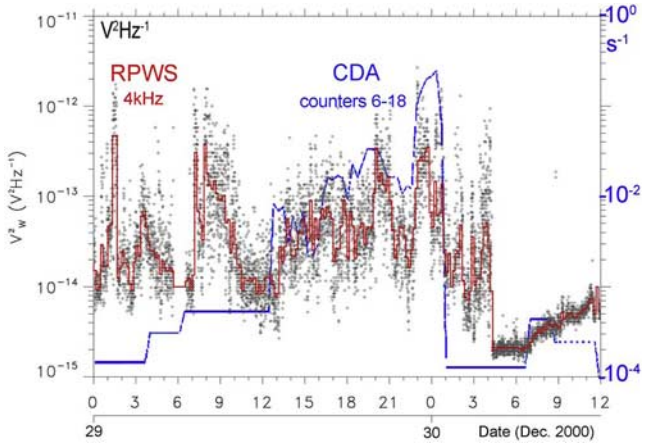

Figure 3. Power spectral density as a function of time at 4 kHz (dots), with 10 min. averages in red, proportional to the dust impact rate, compared to the rate measured with the cosmic dust analyser (blue line, adapted from [*Graps et al.*, 2001]).

was observed in previous dust detections with wave instruments [*Meyer-Vernet*, 2001]. Dust impacts produce such a power spectrum when the rise time of the voltage pulse greatly exceeds $1/(2\pi f)$ - a generic behaviour of the squared Fourier transform [*Aubier et al.*, 1983; *Meyer-Vernet*, 1985]. The observed slope is slightly less steep because the pulse rise time is not much greater than $1/(2\pi f)$, and other contributions are not fully negligible at higher frequencies. For uncorrelated identical impacts, the total power is proportional to the impact rate, and the large observed variability reveals the variability of the impact rate.

[10] On the other hand, in the absence of dust impacts, the signal is the ubiquitous plasma quasi-thermal noise (Figure 2b), produced by quasi-thermal plasma fluctuations near the plasma frequency f_p, which depends on the electron density n and temperature T_e, plus the shot noise of electron impacts and photoelectron emission on the spacecraft and antennas [*Meyer-Vernet and Perche*, 1989]. The latter has a f^{-2} power spectrum because the rise time of pulses due to electrons is smaller than $1/(2\pi f)$; its level varies roughly as the electron flux, so that the variations shown in Figure 2d from Dec.30 to Jan.4 in the range $3-6 \times 10^{-15}$ V^2 Hz^{-1}, reveal the variation of the thermal electron flux, proportional to $nT_e^{1/2}$, as the spacecraft travels in the Jovian magnetosheath, crossing several times the bow shock [*Kurth et al.*, 2002]. At Jupiter, the antenna length on Cassini is too short compared to the ambient Debye length for the quasi-thermal noise to exhibit a significant f_p peak, but unstable Langmuir waves are occasionally observed (e.g., the sporadic f_p line around 3.5 kHz on Figure 1 from Jan 1.0 to Jan 3.5), revealing n, so that the observed noise level can be used to deduce T_e.

[11] Whereas the stationary signal of small spectral index reveals the properties of the ambient plasma, the impulsive noise having a large spectral index reveals dust properties. Figure 3 concentrates on the period when count rates from the on-board dust analyser (CDA) have been published together with dust properties. One sees that when the CDA is oriented adequately and records dust (Dec.29:12h to Dec.30:01h), the wave power (dots, with averages in red) and the dust count rate (blue line, from *Graps et al.* [2001]) vary similarly.

3. Voltage Power Spectrum From Dust Impacts on Cassini

[12] Let us compare the observed wave level with that expected for impacts reported from the dust detector analysis. Joint detections with Cassini and Galileo yielding observing delays between spacecraft, together with calculations of trajectories, were used to determine a particle radius $\simeq$6 nm and density $\simeq$1.35–1.75 g cm^{-3}, whence a mass $m \simeq 10^{-21}$ kg, and a speed $v \simeq 450$ km s^{-1} [*Graps et al.*, 2001].

[13] The electric antennas respond to the charge released by dust grains impacting the spacecraft. Each impact produces an expanding plasma cloud that we model, for an order-of-magnitude estimate, as Q/e electrons and Q/e ions at temperature T expanding at velocity v_E. When the cloud's Debye length becomes greater than its radius, charges decouple, so that the electrons can leave and be recollected by the target (whose electrostatic potential is positive in the absence of dust impacts), whereas the cloud's space charge produces an electric field. This holds until the cloud's density has decreased to the ambient level n, which takes place when the cloud's radius is $R \sim (3Q/(4\pi en))^{1/3}$, at the time

$$\tau \sim (3Q/(4\pi en))^{1/3}/v_E \quad (1)$$

[14] To estimate the corresponding voltage expected on the radio receiver, an important question is whether the pulses are observed in monopole or dipole mode, and whether there is an asymmetry between the signals on the different booms. Figure 4 compares the power at 4 kHz on the monopoles U and V (red and green, respectively) with that on the monopole W, as a function of the latter. One sees that for small signals: $V^2 < 10^{-14}$ V^2 Hz^{-1}, which are produced by the plasma quasi-thermal and shot noise, there is a small but significant difference between booms, which is not surprising since they are not located similarly with respect to the spacecraft wake, and the signal is recorded also by the dipole with a similar order of magnitude. On the other hand, for dust impacts, which show up above a few 10^{-14} V^2 Hz^{-1}, the powers on the three booms are very similar. This is confirmed by the fact that the power on the dipole is extremely small, remaining at the quasi-thermal level when monopoles record dust.

[15] This indicates clearly that the observed pulses are pulses in spacecraft potential, measured in monopole mode because in that configuration the receiver responds to the antenna voltage with respect to that of the spacecraft body. In contrast, in dipole mode, it responds to the difference in signals from the monopoles U and V, so that it does not record the pulses in spacecraft potential, except via a very small common-mode rejection factor.

[16] In addition, measured voltages did not show up drastic changes while orientation of the spacecraft was changing. This indicates that the whole spacecraft area serves as a target, which we shall approximate by an equivalent projected area $S \sim 15$ m^2.

19448007, 2009, 3, Downloaded from https://agupubs.onlinelibrary.wiley.com/doi/10.1029/2008GL036752 by Cochrane France, Wiley Online Library on [21/10/2022]. See the Terms and Conditions (https://onlinelibrary.wiley.com/terms-and-conditions) on Wiley Online Library for rules of use; OA articles are governed by the applicable Creative Commons License

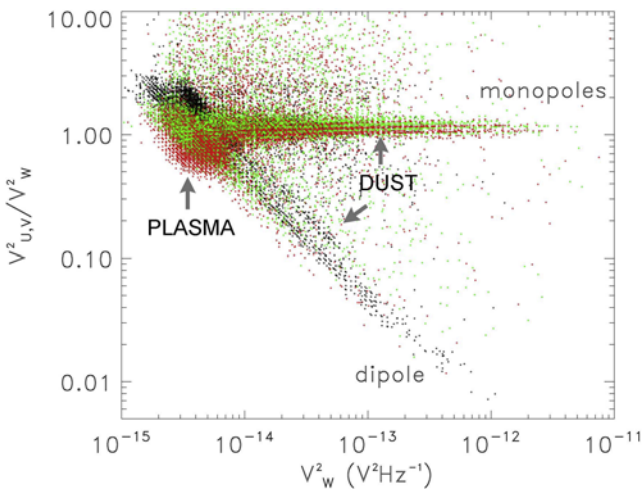

Figure 4. Ratios of the power at 4 kHz on the monopoles U and V (red and green respectively) to that on W, as a function of the latter during the period shown in Figure 2. The ratio of the power on the dipole U-V to that on the monopole W is plotted in black. The dust, which shows up above about a few 10^{-14} V^2 Hz^{-1} is seen on the monopoles with similar levels on each, whereas the dipole records only the (smaller) plasma noise. The remaining points are Jovian electromagnetic emissions, whose relative intensities depend on other factors.

[17] When the spacecraft of capacitance C recollects a charge Q, this produces a pulse in spacecraft potential of amplitude $\delta V \sim Q/C$, which is detected by the monopole antennas. Hence, the power spectrum at frequencies such that $\omega\tau > 1$ is $V^2 \sim 2 < N\delta V^2\tau^{-2} > \Gamma^2/\omega^4$, where the angular brackets stand for an average over impacts of rate N and Γ is the antenna gain [*Meyer-Vernet et al.*, 1996]. Substituting the expression of δV and the impact rate $N \sim FS$ with F the particle flux and S the target's surface, this yields

$$V^2 \sim 2S(\Gamma/C)^2 < F(Q/\tau)^2 > /\omega^4 \qquad (2)$$

[18] Dust impact ionisation involves complex processes not fully included in theory and laboratory simulations, so that the charge Q is determined with a large uncertainty. With the stream speed of 450 km/s reported from the dust analyser observations, each atom (for atomic mass $A \simeq 20$) carries a kinetic energy of 21 keV, which should produce very strong effects, well outside the range presently studied; in that case most of the released material comes from the target, with possible multiple ionisation and production of negative ions. We shall assume that Q varies with the grain's mass and speed according to the typical relationship $Q \simeq 0.7m^{1.02}v^{3.48}$ with Q in Cb, m in kg, v in km s^{-1} [*McBride and McDonnell*, 1999], which also depends on angle of incidence, and grain and target composition. For the reported particles having $m \simeq 10^{-21}$ kg, this yields $Q \sim 5 \times 10^{-13}$ Cb, with an uncertainty of a factor of ten.

[19] The spectral index observed on Dec.29 shows that $\tau \sim 1/(2\pi f)$ at 4 kHz, i.e., $\tau \sim 4 \times 10^{-5}$ s. With the expression (1) of τ, Q estimated above, and the ambient plasma density $n \sim 0.15$ cm^{-3} estimated from the f_p line (Figure 1), this yields $v_E \sim 40$ km/s, compatible with other estimates [*Hornung and Kissel*, 1994]. Substituting in (2) the above values of S, τ, and Q, $C \sim 200$ pF with $\Gamma \simeq 0.4$ [*Gurnett et al.*, 2004], we obtain $V^2 \sim 5 \times 10^{-14}$ F V^2 Hz^{-1} at 4 kHz.

[20] Equating this value to the averaged spectrum at 4 kHz (red line in Figure 3) recorded during the dust analyser detection on Dec.30 around 0h, we find the flux $F \sim 10$ m^{-2} s^{-1}. Even though this estimate is affected by the large uncertainty on the charge Q, it is consistent with the observation that at this time the dust signature is found in all of the wave spectra, meaning that there is always at least one impact during $\Delta t \sim 0.15$ s. This shows that the impact rate $N \gg 7$ s^{-1}, which yields (with $S \simeq 15$ m^2) the constraint on the flux: $F \gg 0.5$ m^{-2} s^{-1}.

4. Discussion

[21] The flux $F \sim 10$ m^{-2} s^{-1} of nanoparticles estimated from the Cassini wave data on 30 December 2000 around 0h is similar to the impact rate reported by the on-board dust analyser at this time; indeed, dividing the CDA impact rate of $\sim$0.2 s^{-1} reported at this time by $S_{DA}\Omega_{DA}/\pi$, with $S_{DA} \simeq 0.1$ and $\Omega_{DA} \simeq 0.6$ ster from *Srama et al.* [2004] yields 10 m^{-2} s^{-1}. It is also in the range of values reported by long-term studies of Jovian dust streams with Galileo, both in amplitude and variability [*Krüger et al.*, 2005].

[22] It is important to keep in mind that since laboratory simulations of impact ionisation have neither been performed with nanoparticles, nor with speeds greater than 100 km/s, our result relies on a huge extrapolation of empirical data, even though it agrees with independent constraints. It is thus at best an-order-of-magnitude estimate. Similarly, the properties of the dust particles reported from the dust analyser measurements are model-dependent. Furthermore, both instruments have very different detecting areas and time scales, so that drawing conclusions from the comparison of their results should involve more detailed studies.

[23] We have not included in our analysis the periods when the on-board magnetosphere imaging instrument (MIMI) is experiencing electric discharges, which may be triggered by nanoparticle impacts on this instrument. In these periods (Dec.29, 5:40–6:35 and Jan.05, after 8:30), the RPWS signal might be contaminated, and, moreover, the wave pulses are detected also in dipole mode, contrary to those analysed here.

[24] A number of similar events have been recorded by Cassini/RPWS, not only near Jupiter and Saturn, but also in the solar wind much closer to the Sun. The latter are under study and may confirm the discovery of fast nanoparticles accelerated by the solar wind at 1 AU made recently with STEREO/WAVES [*Meyer-Vernet et al.*, 2008].

[25] **Acknowledgments.** We acknowledge support by the Centre National d'Etudes Spatiales.

References

Aubier, M. G., N. Meyer-Vernet, and B. M. Pedersen (1983), Shot noise from grain and particle impacts in Saturn's ring plane, *Geophys. Res. Lett.*, *10*, 5–8.

Drapatz, S., and K. W. Michel (1974), Theory of shock-wave ionization upon high-velocity impact of micrometeorites, *Z. Naturforsh. A*, *29*, 870–879.

19448007, 2009, 3, Downloaded from https://agupubs.onlinelibrary.wiley.com/doi/10.1029/2008GL036752 by Cochrane France, Wiley Online Library on [21/10/2022]. See the Terms and Conditions (https://onlinelibrary.wiley.com/terms-and-conditions) on Wiley Online Library for rules of use; OA articles are governed by the applicable Creative Commons License

Göller, J. R., and E. Grün (1989), Calibration of the Galileo/Ulysses dust detectors with different projectile materials and at varying impact angles, *Planet. Space Sci.*, *37*, 1197–1206.

Graps, A. L., E. Grün, H. Svedhem, H. Krüger, M. Horányi, A. Heck, and S. Lammers (2000), Io as a source of the Jovian dust streams, *Nature*, *405*, 48–50.

Graps, A. L., E. Grün, H. Krüger, M. Horányi, and H. Svedhem (2001), Io revealed in the Jovian Dust Streams, in *Proceedings of the Meteoroids 2001 Conference*, edited by B. Warmbein, *Eur. Space Agency Spec. Publ.*, *ESA SP-495*, 601–608.

Grün, E., et al. (1992), Ulysses dust measurements near Jupiter, *Science*, *257*, 1550–1552.

Gurnett, D. A., et al. (2004), The Cassini radio and plasma wave investigation, *Space Sci. Rev.*, *114*, 395–463.

Horányi, M., E. Grün, and A. Heck (1997), Modeling the Galileo dust measurements at Jupiter, *Geophys. Res. Lett.*, *24*, 2175–2178.

Hornung, K., and J. Kissel (1994), On shock wave impact ionization of dust particles, *Astron. Astrophys.*, *291*, 324–336.

Johnson, T. V., G. Morfill, and E. Grün (1980), Dust in Jupiter's magnetosphere: An Io source?, *Geophys. Res. Lett.*, *7*, 305–308.

Krüger, H., G. Linkert, D. Linkert, R. Moissl, and E. Grün (2005), Galileo long-term dust monitoting in the Jovian magnetosphere, *Planet. Space Sci.*, *53*, 1109–1120.

Kurth, W. S., et al. (2002), The dusk flank of Jupiter's magnetosphere, *Nature*, *415*, 991–994.

Kurth, W. S., T. F. Averkamp, D. A. Gurnett, and Z. Wang (2006), Cassini RPWS observations of dust in Saturn's E ring, *Planet. Space Sci.*, *54*, 988–998.

McBride, N., and J. A. M. McDonnell (1999), Meteoroid impacts on spacecraft: Sporadics, streams, and the 1999 Leonids, *Planet. Space Sci.*, *47*, 1005–1013.

Meyer-Vernet, N. (1985), Comet Giacobini-Zinner diagnosis from radio measurements, *Adv. Space Res.*, *5*, 37–46.

Meyer-Vernet, N. (2001), Detecting dust grains with electric sensors: Planetary rings, comets, and the interplanetary medium, in *Proceedings of the 7th Spacecraft Charging Technology Conference*, edited by R. A. Harris, *Eur. Space Agency Spec. Publ.*, *ESA SP-476*, 635–640.

Meyer-Vernet, N., and C. Perche (1989), Toolkit for antennae and thermal noise near the plasma frequency, *J. Geophys. Res.*, *94*, 2405–2415.

Meyer-Vernet, N., A. Lecacheux, and B. M. Pedersen (1996), Constraints on Saturn's E ring from the Voyager-1 radioastronomy instrument, *Icarus*, *123*, 113–128.

Meyer-Vernet, N., S. Hoang, K. Issautier, M. Maksimovic, R. Manning, M. Moncuquet, and R. Stone (1998), Measuring plasma parameters with thermal noise spectroscopy, in *Measurement Techniques in Space Plasmas: Fields, Geophys. Monograph Ser.*, vol. 103, edited by R. Pfaff et al., pp. 205–210, AGU, Washington, D. C.

Meyer-Vernet, N., et al. (2008), Voltage pulses on STEREO/WAVES: Nanoparticles picked-up by the solar wind?, *Eos Trans. AGU*, *89*, Fall Meet. Suppl., Abstract SH13B-1545.

Scarf, F. L., D. A. Gurnett, W. S. Kurth, and R. L. Poynter (1982), Voyager-2 Plasma wave observations at Saturn, *Science*, *215*, 587–594.

Srama, R., et al. (2004), The Cassini Cosmic Dust Analyzer, *Space Sci. Rev.*, *114*, 465–518.

Warwick, J. W., et al. (1982), Planetary radioastronomy observations from Voyager-2 near Saturn, *Science*, *215*, 582–586.

Zook, H. A., et al. (1996), Solar wind magnetic field bending of Jovian dust trajectories, *Science*, *274*, 1501–1503.

D. A. Gurnett, Department of Physics and Astronomy, University of Iowa, Iowa City, IA 52242, USA.

M. L. Kaiser, NASA Goddard Space Flight Center, Greenbelt, MD 20771, USA.

A. Lecacheux and N. Meyer-Vernet, LESIA, Observatoire de Paris, CNRS, Université Paris Diderot, 5 Place Jules Janssen, F-92190 Meudon CEDEX, France. (nicole.meyer@obspm.fr)

19448007, 2009, 3, Downloaded from https://agupubs.onlinelibrary.wiley.com/doi/10.1029/2008GL036752 by Cochrane France, Wiley Online Library on [21/10/2022]. See the Terms and Conditions (https://onlinelibrary.wiley.com/terms-and-conditions) on Wiley Online Library for rules of use; OA articles are governed by the applicable Creative Commons License